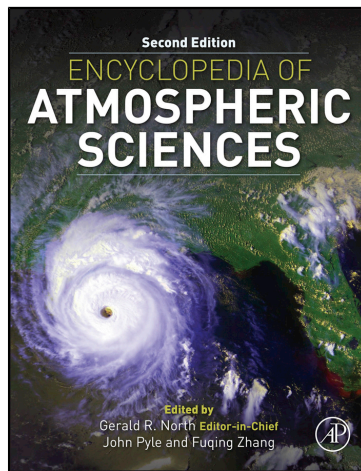


**Provided for non-commercial research and educational use only.
Not for reproduction, distribution or commercial use.**

This article was originally published in the book *Encyclopedia of Atmospheric Sciences*, 2nd edition. The copy attached is provided by Elsevier for the author's benefit and for the benefit of the author's institution, for non-commercial research, and educational use. This includes without limitation use in instruction at your institution, distribution to specific colleagues, and providing a copy to your institution's administrator.



All other uses, reproduction and distribution, including without limitation commercial reprints, selling or licensing copies or access, or posting on open internet sites, your personal or institution's website or repository, are prohibited. For exceptions, permission may be sought for such use through Elsevier's permissions site at: <http://www.elsevier.com/locate/permissionusematerial>

From Grotjahn, R., 2015. Energy Cycle. In: Gerald R. North (editor-in-chief), John Pyle and Fuqing Zhang (editors). *Encyclopedia of Atmospheric Sciences*, 2nd edition, Vol 3, pp. 51–64.

ISBN: 9780123822253

Copyright © 2015 Elsevier Ltd. unless otherwise stated. All rights reserved.
Academic Press

Energy Cycle

R Grotjahn University of California, Davis, CA, USA

© 2015 Elsevier Ltd. All rights reserved.

Synopsis

The energy cycle provides a physically meaningful system to understand several constraints upon and properties of the general circulation. Energy is conserved and it can be tracked even as it changes from one form to another. Energy properties can be analyzed to deduce the net circulations as well as the rates at which the circulations are created, maintained, or destroyed.

Introduction

The total energy per unit mass (TE) is defined as:

$$\underbrace{C_p T + gZ + Lq}_{\text{MSE}} + \underbrace{\frac{1}{2}(u^2 + v^2 + w^2)}_{\text{KE}} = \text{TE} \quad [1]$$

where C_p is the specific heat at constant pressure, T the temperature, g the acceleration of gravity, Z the geopotential height, L the latent heat of vaporization or sublimation, q the specific humidity, and (u, v, w) the eastward, northward, and upward wind components, respectively. The terms above are internal energy at constant pressure, gravitational energy, latent energy from phase changes of water, and kinetic energy (KE) per unit mass, respectively. Together the first two terms define dry static energy (DSE) while including the third defines moist static energy (MSE).

The distributions of MSE and DSE in summer and winter seasons are shown in [Figure 1](#). The DSE monotonically increases with height because the large-scale atmosphere is statically stable. DSE decreases toward the poles due to cooler temperatures. The addition of moisture, with most moisture mass in the lower troposphere, causes the vertical derivative of MSE to reverse sign (implying convective potential instability) in the lower tropical troposphere and causes the contours to be nearly vertical in the midlatitude troposphere (the latter indicative of a nearly moist adiabatic lapse rate). In the horizontal, higher values of MSE favor the tropical and summer continents as well as the intertropical and other convergence zones (indicative of low-level moisture convergence). In middle latitudes, lower values of MSE occur on the colder east sides of the continents.

Potential energy (PE) is related to DSE. PE is useful for global energy balance. A tiny fraction of the PE, called the available potential energy (APE), is usable to drive the KE. APE is defined as the difference between the PE and the minimum PE that could be achieved by an adiabatic rearrangement of mass. APE is used to understand the links between PE and KE. Sometimes latent heating is included directly in the APE, usually it is treated as a separate diabatic process.

Solar radiant energy does not reach the Earth equally everywhere. On an annual average, the tropics receive and

absorb far more solar energy than the polar regions. This distribution of absorbed energy creates an uneven distribution of temperature. Temperature, pressure, and density are related, so the PE has an uneven distribution too. The existence of APE is essentially due to the horizontal variations in density and temperature. A portion of the APE is converted into motions (KE) as the atmosphere tries to remove these density and temperature variations. The motions redistribute some mass, but mainly the atmosphere transports heat. The atmospheric circulation becomes a complex balance between radiant energy input and output that create APE, which is needed to generate the KE of circulations that in turn strive to create a state of no APE.

APE and KE are defined in formal mathematical ways. The mathematics show interactions from which physical mechanisms (like baroclinic instability) can be identified. The energy equations describe the following chain of events: radiation creates APE; some APE is converted into motions that redistribute the heat energy; and KE in turn is lost by conversion back to APE and by friction. The forms of energy and the *net* conversions between them can be represented via a 'box' diagram. However, the box diagram does not show the energy cycle in an intuitive sense. To make the physical mechanisms clear, energy must be examined regionally and one phenomenon at a time.

Conceptual Models

Two-Fluid Model

A fluid flow analog of the pendulum illustrates forms and conversions of energy. Imagine a tank holding two immiscible fluids of different densities, separated by a vertical barrier ([Figure 2\(a\)](#)). The initial state has the highest center of mass and thus greatest gravitational PE. If the barrier is suddenly removed, the fluids begin to move. The motion accelerates until the point in time where the greatest amount of the denser fluid underlies the greatest amount of the less dense fluid ([Figure 2\(b\)](#)). The center of mass is now lowest as is the gravitational PE. Ignoring friction, mixing, and turbulent effects, KE is maximized at this point. As time proceeds further, the fluids overshoot this state and KE begins converting back to PE ([Figure 2\(c\)](#)).

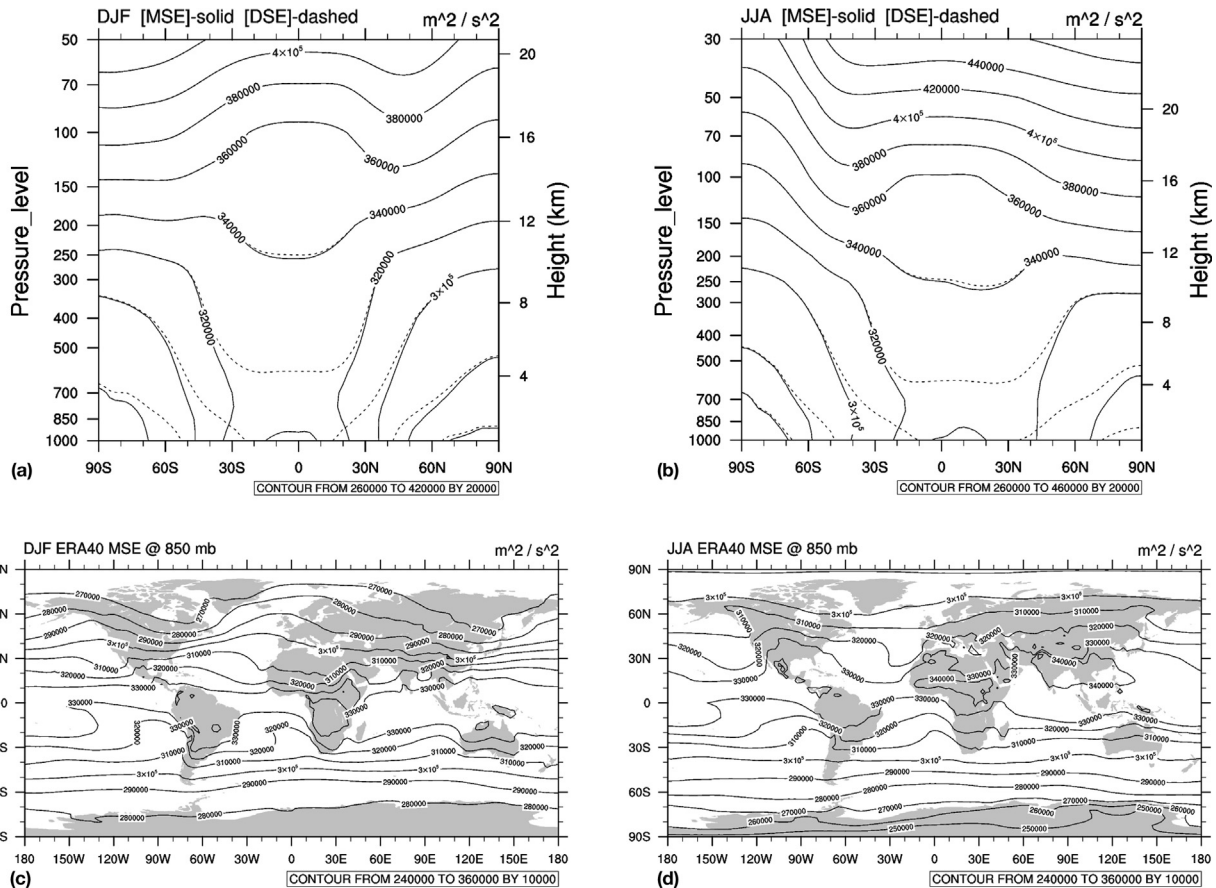


Figure 1 Distributions of DSE and MSE during December–February (left column) and June–August (right column) extreme seasons. In (a) and (b), solid lines are MSE while dashed lines are DSE, which differ mainly in the lower and tropical troposphere. In the deep tropics, the vertical gradient of MSE reverses sign from lower to upper troposphere. In (c) and (d), the longitudinal distribution of MSE is illustrated using the pattern at 850 hPa. ERA-40 reanalysis data from 1979 to 2001 used were provided by the European Centre for Medium Range Weather Forecasts.

APE is defined as the difference between the current PE and the minimum PE. The state with lowest PE is the ‘reference state’ having zero APE. The reference state definition is somewhat arbitrary. Another mechanism could possibly occur at some later time to lower further the minimum PE, for example, a net temperature decrease. However, the size of the conversions, generation, and destruction are less arbitrary. APE is intended to represent PE available for driving motions, so the reference state is usually defined by adiabatically rearranging

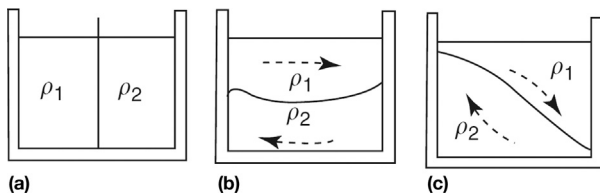


Figure 2 Schematic model of fluid motion illustrating APE and KE concepts. The tank holds two immiscible fluids with density $\rho_1 < \rho_2$. (a) Initial state; (b) state with maximum KE but minimum PE reached during the first oscillation; and (c) state where KE is being converted back to PE.

atmospheric properties so as to reach a state of minimum PE. This model reveals that density differences across a fixed elevation in the tank are proportional to the APE.

This model relates to the atmosphere as follows:

1. Temperature differences create the density differences. The less dense fluid represents the tropics; the denser fluid represents polar regions.
2. The reference state has minimum center of mass when the air ‘layers’ are flat. However, flat fields of pressure and temperature imply no geostrophic winds and remove a driver for ageostrophic winds.
3. Horizontal density differences (manifest as sloping fluid layers) have APE but also produce horizontal pressure gradients that accelerate the air. On the rotating Earth, geostrophic winds and thus KE are present, too. So, reservoirs, sources, and sinks of APE are not independent of KE.

Carnot Cycle

A Carnot cycle analysis can estimate KE generation from thermodynamic changes that an air parcel undergoes

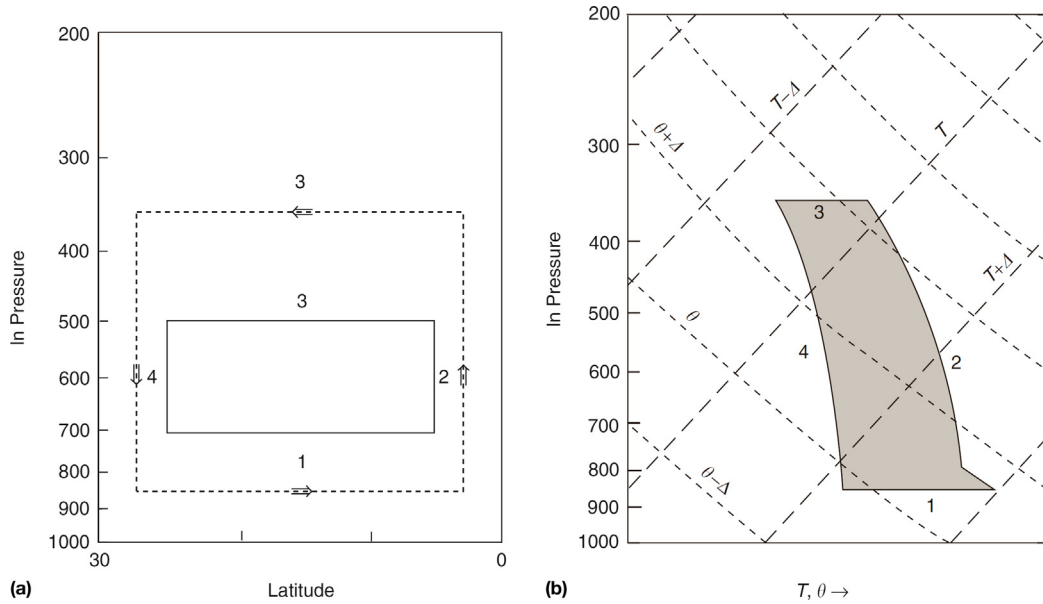


Figure 3 Interpretation of the Hadley circulation as a Carnot cycle. (a) Meridional cross section showing the idealized circulation. The dashed line shows an average path followed by the parcels with numeric labels for each leg. (b) Skew T-lnP plot of the thermodynamic changes along each of the four legs drawn in part (a). The shaded area is proportional to the energy converted from PE to KE.

while completing an atmospheric circuit. The Hadley cell is a conceptual model for the zonal mean tropical circulation. Air in the lower troposphere moves equatorward while gaining heat and moisture from surface fluxes. Near the equator, rapid ascent within thunderstorms releases and advects much latent heat energy. Reaching the upper troposphere, air moves poleward, cools radiatively, and sinks, completing a circuit.

KE generation can be estimated by plotting the thermodynamic properties of air parcels on a skew T-lnP chart. A unit area anywhere on the chart corresponds to a specific amount of energy exchange. Figure 3 shows a possible circuit around an annual mean Hadley cell. The amount of APE converted into KE by a kilogram of air while it completes the plotted circuit is $E \sim 1.4 \times 10^3 \text{ J kg}^{-1}$.

The rate of energy release per unit horizontal area, R , by all the air in motion can be compared with the rate per unit area of energy absorbed from the Sun.

$$R = ME t^{-1} A^{-1} \quad [2]$$

where M is the mass in motion, t is the time to complete the circuit, and A is the area of the Hadley cell. For the schematic circulation indicated in Figure 3(a), $M \sim 10^{18} \text{ kg}$, $A \sim 10^{14} \text{ m}^2$, and $t \sim 3 \times 10^6 \text{ s}$. The total rate of energy released by the Hadley cell is $ME t^{-1} \sim 5 \times 10^{14} \text{ J s}^{-1}$. However, the rate per unit area is only $R \sim 3.6 \text{ W m}^{-2}$. The absorbed solar radiation in the tropics is 100 times larger than R , making the atmosphere an 'inefficient' heat engine. (Efficiency of the Carnot cycle is often measured in a way dependent on the temperature difference during the cycle, but this estimate is related to energy input.)

The model has the following properties:

1. Warmer air is rising and cooler air is sinking, so the center of mass is lowered and KE is created; the circuit is counterclockwise and the circulation is 'thermally direct'. In contrast, the Ferrel cell is a clockwise circuit that reduces KE to increase PE.

2. A steady state is reached if the frictional losses balance the KE generation.
3. The rate of KE generation depends on the area enclosed by the circuit divided by the time to complete the circuit. That time depends on the speed of parcels, a point reinforced later when the APE to KE conversion term is considered.
4. The amount of energy converted is proportional to a circuit integral of temperature, so it increases as the temperature difference increases between the warm and cold stages of the cycle. During winter the meridional temperature gradient is stronger than summer, and so is the Hadley cell.
5. In winter, the air motion of the Hadley cell is five to seven times stronger than the Ferrel cell, but larger temperature differences occur along the Ferrel circuit. So, the net energy conversions are similar (see Energy Box Diagram section below).
6. Large energies are involved, but only a tiny fraction of the solar radiation actually drives the observed motions.
7. The path followed by air parcels was specified, not predicted.

Available Potential Energy

DSE and therefore PE combine both gravitational and internal energies. To the extent that hydrostatic balance and ideal gas law are valid and working at constant volume, then:

$$\begin{aligned} PE &= \int_0^\infty \rho g Z dz + \int_0^\infty \rho C_V T dz = \int_0^{P_s} Z dP + \int_0^\infty \rho C_V T dz \\ &= \int_0^\infty \rho (R + C_V) T dz = \int_0^\infty \rho C_P T dz \end{aligned} \quad [3]$$

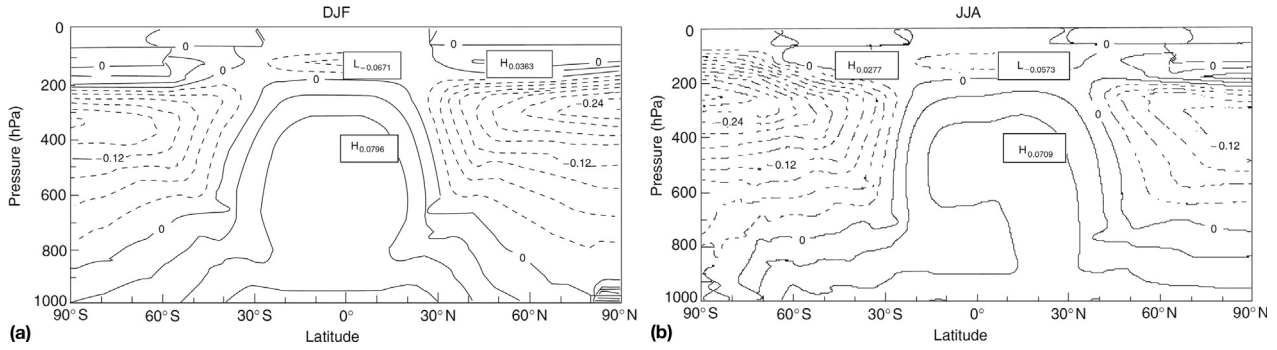


Figure 4 Zonal mean efficiency factor [ϵ] for (a) December–February and (b) June–August. [ϵ] is estimated from zonal mean 1979–99 National Center for Environmental Prediction/National Center for Atmospheric Research (NCEP/NCAR) reanalysis data. The contour interval is 0.03.

Hence, gravitational and internal energies are bound together in an R/C_p ratio. APE is approximated by temperature variations on a pressure surface.

$$\begin{aligned} \text{APE} &= \int \epsilon C_p T \, dM \approx \frac{1}{2} \kappa C_p P_{00}^{-\kappa} \\ &\times \int P^{\kappa-1} \{ \theta - \bar{\theta} \}^2 \left(\frac{\partial \theta}{\partial P} \right)^{-1} dM \end{aligned} \quad [4]$$

$$\epsilon = 1 - \left(\frac{P_r}{P} \right)^\kappa \quad [5]$$

M is the mass while other variables are potential temperature θ , $P_{00} = 10^5$ Pa, specific heat at constant pressure C_p , $\kappa = RC_p^{-1}$, ideal gas constant R , and ‘efficiency factor’ ϵ . $P_r(\theta)$ is the reference pressure: the average pressure on a potential temperature surface θ . APE is zero when $P = P_r$ everywhere in the domain. The overbar denotes the horizontal average on an isobaric surface. APE has the following properties:

1. For an integral over the depth of the atmosphere, APE differs from PE by the factor ϵ .
2. Observed PE is about a thousand times greater than estimates of global average APE.
3. Hemispheric PE is greater in summer since the air is generally warmer than in winter.
4. Hemispheric APE is greater in winter when the meridional temperature gradient is stronger making the $\{ \}$ term larger than in summer. The larger the atmosphere departs from the reference state mean, the larger the magnitude of ϵ becomes.
5. Diabatic heating or cooling can create APE if it magnifies the departures from the reference state, but the same heating or cooling can destroy APE if it reduces the departures. In simplistic terms, APE is generated by ‘heating where it is hot or cooling where it is cold’.
6. $\epsilon > 0$ in ‘hot’ regions and $\epsilon < 0$ in ‘cold’ regions. From **Figure 4**, ϵ has a positive maximum in the tropical middle troposphere and negative minimums in high latitudes. In middle latitudes, the sign varies with longitude: $\epsilon > 0$ over oceans during winter or warm sectors of frontal cyclones while $\epsilon < 0$ over continents in winter or behind cold fronts.

Kinetic Energy

KE is primarily contained in horizontal winds:

$$\text{KE} = \frac{1}{2} (u^2 + v^2) \, dM \quad [6]$$

KE has the following properties:

1. The distribution of zonal mean KE (**Figure 5**) has maximums at upper levels near the subtropical jets.
2. KE is related to atmospheric momentum and torque. Momentum fluxes by the Hadley cells and by midlatitude eddies maintain the KE maximum near the subtropical jet. Slowing down surface easterlies in the Hadley circulation imparts westerly momentum that is transported to higher latitudes by the upper branch of the Hadley Cell. Eddy momentum flux convergence is another source.

Energy Generation and Conversion

Energy Equations

To understand how energy evolves one needs formulae for APE and KE tendencies in a limited domain. The domain may be a unit area in the meridional plane (useful for calculating zonal means) or enclosing a single phenomenon to the exclusion of others (e.g., a single frontal cyclone). Tendency equations for APE and KE in a mass M between two isobaric surfaces are

$$\begin{aligned} \frac{\partial \text{APE}}{\partial t} &= \underbrace{\int (\epsilon q) dM}_a + \underbrace{\int (\epsilon \omega \alpha) dM}_b - \underbrace{\int \epsilon (\nabla_p \cdot (V_p C_p T)) dM}_c \\ &+ \underbrace{\int \left(C_p T \frac{\partial \epsilon}{\partial t} \right) dM}_d \end{aligned} \quad [7]$$

$$\frac{\partial \text{KE}}{\partial t} = - \underbrace{\int (V_p \cdot F) dM}_a - \underbrace{\int (V_p \cdot \nabla_p \Phi) dM}_b - \underbrace{\int (\nabla_p \cdot (V_p \text{KE})) dM}_c \quad [8]$$

where q contains all diabatic heating and F is the frictional force. Also, ω is the pressure coordinate (‘vertical’) velocity, α is

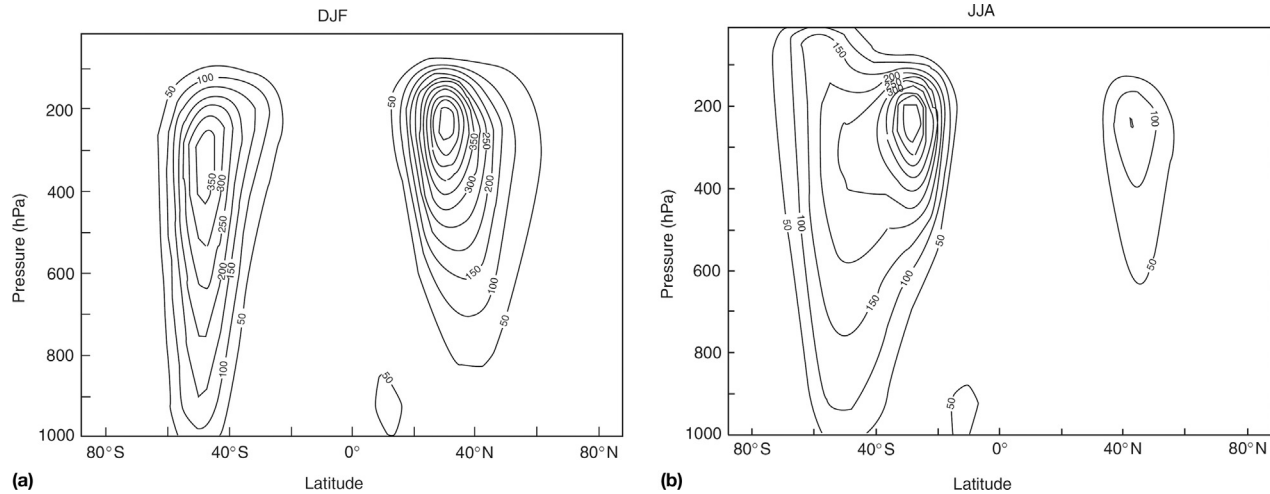


Figure 5 Zonal mean KE density for (a) December–February and (b) June–August using 1979–99 NCEP/NCAR reanalysis data. The contour interval is $50 \text{ kg s}^{-2} \text{ m}^{-1}$.

the specific volume, Φ is the geopotential, and P subscript indicates evaluation on isobaric surfaces.

The terms are ordered to match similar processes. Term 'a' in each equation has diabatic source/sink mechanisms. Term 'b' is similar but has opposite sign in the APE and KE equations and so represents a (baroclinic) conversion between these two forms of energy. Term 'c' is divergence of PE or KE flux; it is a conversion between the APE or KE inside and that external to the domain; and baroclinic or barotropic conversions, respectively, appear in this term.

Diabatic Sources and Sinks of Energy

There are five categories of diabatic processes: solar and terrestrial radiation, latent and sensible surface heat flux, and friction. **Figure 6** illustrates how diabatic heating is distributed on the seasonal and zonal means.

1. Solar radiation absorbed. Over much of the atmosphere the emission exceeds the absorption (net radiative cooling

(NRC) in **Figure 6**) but in the tropical and summer portions of the stratosphere there is net solar absorption (NRH).

2. Terrestrial radiation emitted. NRC (**Figure 6**) is very strong in the winter high latitudes and subtropics through the depth of the atmosphere. The net cooling is strong in the Southern Hemisphere subtropics in summer. Since emission is stronger from lower (warmer) cloud tops, the net cooling increases toward lower subtropical elevations. While the terrestrial emission ($q < 0$) is greater in the tropics, suggesting destruction of APE, the bulk of the net cooling in the diabatic heating field is in the winter hemisphere. APE is generated because the stronger net emission in high latitudes is from cloud tops where ϵ is strongly negative. In the less cloudy subtropical latitudes emission mainly occurs where ϵ has smaller magnitude.

3. Latent heat release. Some solar radiation absorbed by the Earth's surface evaporates water. Evaporation introduces water vapor into the atmosphere, primarily in the subtropics. The latent heat is released some distance away where

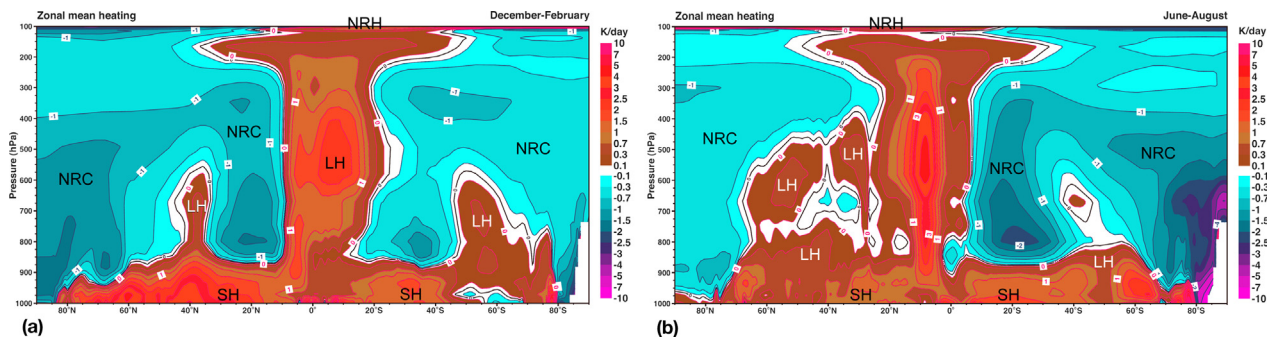


Figure 6 Zonal mean heating calculated as a residual in the temperature conservation equation. Areas near zero have no shading. Areas where shading darkens as values become larger in magnitude are negative values (cooling, 'blue' if in color). Areas where shading becomes lighter as values become larger are positive (heating, 'warm colors' if in color). Labels indicate the processes that tend to be larger in given regions. NRC indicates net radiative cooling, NRH means net radiative heating, LH indicates latent heating, SH indicates surface sensible heat flux mixed upward in the boundary layer. Units are Kelvin perday. Reproduced from Källberg, P., Berrisford, P., Hoskins, B., et al. 2005. European Centre for Medium Range Weather Forecasts (ECMWF) ERA-40 Publication 19: The ERA-40 Atlas, 191 pp.

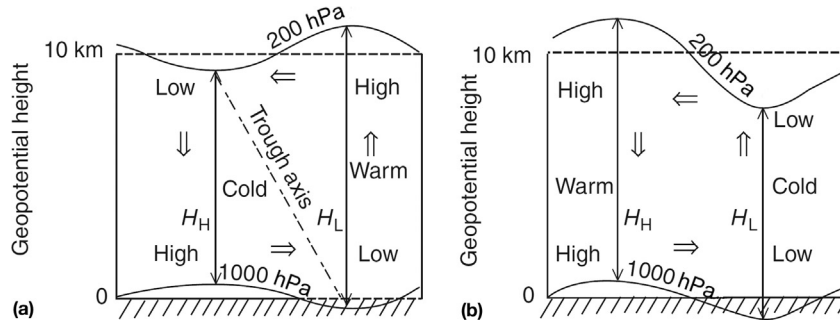


Figure 7 Highly idealized schematic illustration of a midlatitude frontal cyclone during (a) baroclinic growth and (b) baroclinic decay. The 1000 and 200 hPa surfaces are marked. Areas of relatively warmer and colder air at an isobaric level are noted. Double-shafted arrows indicate the relevant part of the ageostrophic circulation. The dot-dashed line in (a) shows the trough axis through the troposphere.

condensation occurs. In the tropics, much latent heat is released in the middle troposphere (mainly in the inter-tropical convergence zone (ICZ)) where $\varepsilon > 0$, hence creating APE. Moisture from the subtropics as well as evaporation over warm waters of an oceanic western boundary current (WBC; e.g., the Gulf Stream) is transported poleward and feeds precipitation in the midlatitude storm tracks. So midlatitude secondary maxima of latent heating occur in the lower and middle troposphere. The midlatitude latent heating is more apparent in summer because the opposing NRC is much stronger in winter. The Asian summer monsoon is seen as a heating maximum near 30° N in **Figure 6(b)**.

4. Surface sensible heat flux. Solar radiation absorbed by the Earth's surface also heats up the ground and that is mixed into the air by turbulent processes. The transfer of sensible heat is large in the subtropics and also near midlatitude WBCs. Generally, the sensible heating is where $\varepsilon > 0$, thereby creating APE. Sensible heating is input into the cold air sector of the extratropical cyclone, thus destroying the temperature contrast between the warm and cold sectors, and so indicating APE destruction. However, sensible heating in the cold sector does lower the static stability, which allows vertical motions to proceed more freely encouraging baroclinic conversion.
5. Friction is only important for KE and it always destroys KE.

Baroclinic Conversions

Terms 'b' in eqns [7] and [8] are similar though opposite in sign, thereby indicating conversion between APE and KE in the limited volume energy equations. Using the hydrostatic and continuity equations:

$$\vec{\nabla}_P \cdot \nabla_P \Phi = \omega \alpha + \nabla_3 \cdot (\vec{V}_3 \Phi) \quad [9]$$

For a closed system, there is no mass divergence and the pressure work term ($\nabla_3 \cdot (\vec{V}_3 \Phi)$) vanishes when integrated over the domain. A large fraction of the wind is described by the geostrophic wind and since the geostrophic wind is proportional to the cross product of Φ , the geostrophic wind does not contribute to the left-hand side of eqn [9]. Hence, ageostrophic motions across geopotential height contours contribute to the left-hand side. For an open system, $\vec{V}_P \cdot \nabla_P \Phi \ll \nabla_3 \cdot (\vec{V}_3 \Phi)$ and so there must be partial cancelation with the $\omega \alpha$ term to have the right-hand side also small. $\vec{V}_3 \Phi$ is a flux of geopotential that

can transport (gravitational) PE into or out of a region. Since $\varepsilon \ll 1$, $\varepsilon \omega \alpha$ has comparable magnitude as $\vec{V}_P \cdot \nabla_P \Phi$.

Two approximate forms of this conversion aid interpretation of the process. For a closed system illustrated in **Figure 7**, the conversion depends on the difference in thickness above the surface high (H_H) versus above the surface low (H_L):

$$-S g |\omega| (H_H - H_L) \sim \int \vec{V}_P \cdot \nabla_P \Phi \, dM \quad [10]$$

S is the horizontal area for each half of the domain and $|\omega|$ is the magnitude of the mean ω . Since thickness is proportional to the mean temperature of the layer of air, the sign and magnitude of the conversion depend on vertical motion in relatively warmer and colder regions. In **Figure 7(a)**, warm air over the surface low rises while cold air sinks, which means $H_L > H_H$ resulting in cyclogenesis (APE \rightarrow KE). In **Figure 7(b)**, warm air overlies the surface high, so it has greater thickness than the air over the low resulting in cyclolysis. The magnitude of the conversion during the developing stage exceeds that during the decay stage implying net generation of KE.

A simple description of the baroclinic conversion is 'warm air rising or cold air sinking converts APE into KE'. The relationship is seen in the quasigeostrophic system, where

$$-\omega \alpha \approx g \mu \omega \theta \quad [11]$$

and $\mu \ll 1$ is a nondimensionalizing constant. The Carnot cycle model illustrates this mechanism as does the A_Z to K_Z conversion found in the tropical Hadley cells. (A_Z is the APE constructed from zonal mean quantities and K_Z is the KE constructed from zonal mean winds.)

For the Hadley cell, the integrand of term b in eqn [8] can be approximated by $-[v] \frac{\partial[\Phi]}{\partial y}$ if one neglects zonally varying phenomena like the Asian Monsoon and the Walker Cell. There is no zonal component because the geopotential term is averaged around a latitude circle and identically zero (if no topography is intercepted, i.e., if there is no mountain torque). The low-level flow in the Hadley cell is down the gradient of geopotential (from higher to lower Φ), so the term (including the minus sign) is positive and thereby generating zonal mean KE. For the upper level generally poleward return flow, both the meridional wind and the Φ gradient reverse sign and the KE are being created. Consistently, the rising ($\omega < 0$) branch of the

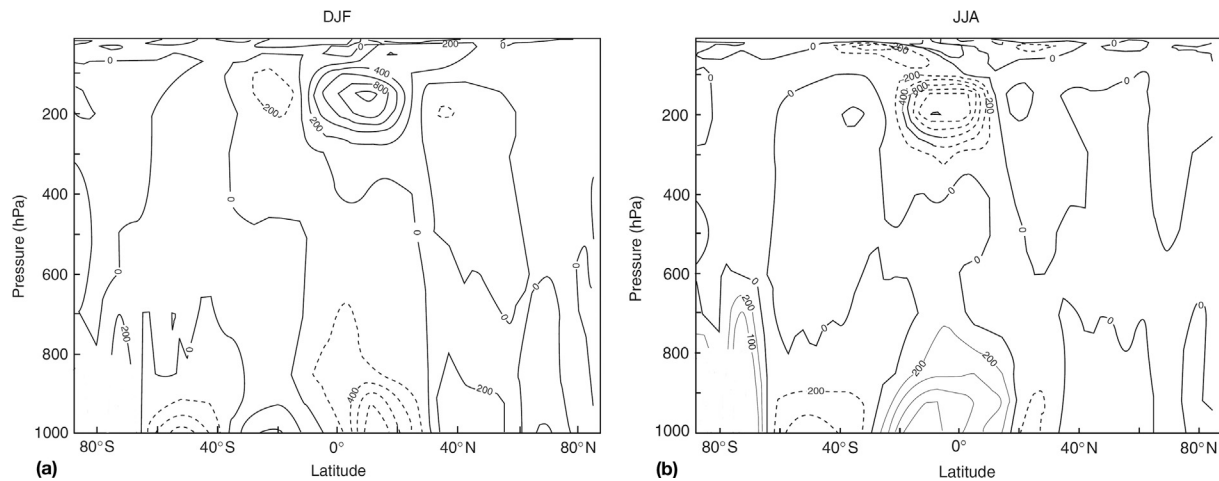


Figure 8 Zonal mean meridional flux of potential temperature $[v\theta]$ for (a) December–February and (b) June–August using 1995–99 NCEP/NCAR reanalysis data. Hadley cell fluxes are apparent in the tropics, while eddy fluxes predominate in midlatitudes.

Hadley cell occurs in the warmer air ($\varepsilon > 0$), so term b in eqn [7] is negative and APE is being lost. Assuming that half the KE conversion takes place in a 300 hPa deep lower layer, moving at 3.5 m s^{-1} , with a geopotential height gradient of 10^{-4} , the full KE conversion in eqn [8] is 2.1 W m^{-2} . The results are consistent with the Carnot cycle calculation and indicate that the KE conversion is small relative to the solar absorption.

In middle latitudes zonally varying phenomena (eddies) dominate the circulation. To drive midlatitude eddies, two conversions are incorporated into the ‘baroclinic’ conversion label: A_Z to A_E and A_E to K_E . In the quasigeostrophic context, the latter is proportional to a vertical eddy heat flux while the former is proportional to a horizontal eddy heat flux. From thermal wind balance, the environment has a meridional temperature gradient and westerly vertical shear. Eddy horizontal heat fluxes are directed down the temperature gradient (toward the pole) if the eddy tilts against the vertical shear. The upstream tilt and vertical heat flux are both visible in the schematic diagram (Figure 7(a)) of cyclogenesis.

Figure 8 shows the observed zonal mean heat flux by all motions. In the tropics the heat flux follows the Hadley cell: lower-level equatorward heat flux and upper-level poleward heat flux. Because MSE is larger at the higher elevation (Figure 1) each Hadley cell has a net poleward heat flux. At higher latitudes heat is advected poleward, mainly in the lower troposphere. The midlatitude eddies have sizable poleward heat flux in the lower troposphere and somewhat less poleward flux in the upper troposphere. The mean meridional (Ferrel) cell circulation opposes the upper troposphere eddy flux and reinforces the lower troposphere eddy flux making the net $[v\theta]$ flux larger in the lower troposphere.

Intra-KE (Barotropic) Conversion

The barotropic conversion rearranges KE. A commonly shown redistribution is between zonal mean and eddy KE. In the KE tendency eqn [8] this conversion (term c) appears as a boundary flux that is zero for a closed domain. The term originates from the horizontal advection terms in the original

component momentum equations and when one derives the conversion between zonal mean and eddy KE then the term is related to eddy momentum flux convergence as well as the mean flow horizontal shear. Zonal mean KE is generated from eddy KE where eddy momentum fluxes are up the gradient of the mean flow.

The eddy momentum fluxes, meridional cells, and jets are linked in the barotropic mechanism. Meridional momentum transport (Figure 9) tends to be largest in the upper troposphere. One reason for this is that midlatitude eddy momentum transport becomes stronger as frontal cyclones reach a mature stage. Momentum transport by the Hadley cell is up the gradient of the zonal mean zonal wind toward the subtropical jet stream; the poleward moving air contains large angular momentum that causes air parcels to accelerate relative to the Earth’s surface. The meridional cells have little meridional motion at the subtropical jet, but the eddies carry momentum further poleward. The Ferrel cell momentum flux opposes the flux by the eddies in the upper troposphere.

Complexity arises from several sources.

1. The eddies have preferred regions of genesis and decay and their momentum fluxes vary greatly between these regions.
2. Mature lows migrate to the cold side of the jet and thus deflect the jet stream equatorward.
3. Eddy momentum fluxes build vertical shear while the eddy heat fluxes reduce the temperature gradient, a combination that destroys thermal wind balance. One consequence is the formation of a secondary circulation, appearing as the ‘Ferrel cell’ on a zonal average, which partially opposes the eddy heat and momentum fluxes. So, the jet streams are equatorward of where the eddy momentum flux has greatest convergence. This Ferrel cell brings westerly momentum downward.
4. The momentum flux convergence in Figure 9 is largest in the winter hemisphere between 30 and 40° N in the upper troposphere. This location of momentum convergence thus seems to be poleward of the subtropical jet. The jet and momentum convergence positions match better if one

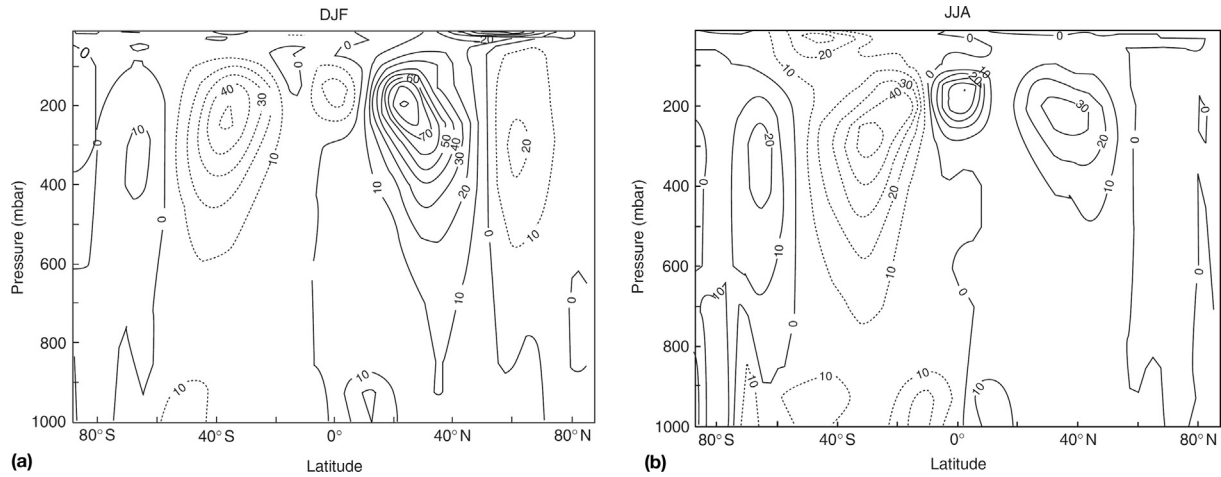


Figure 9 Zonal mean meridional flux of zonal wind $[vu]$ for (a) December–February and (b) June–August using 1995–99 NCEP/NCAR reanalysis data. Hadley cell fluxes are apparent in the tropics, while eddy fluxes predominate in midlatitudes.

accounts for the spherical geometry. The zonal component of zonal mean KE tendency is given by eqn [12]:

$$\frac{\partial}{\partial t} \int \left(\frac{[u]^2}{2} \right) dm = - \underbrace{\int [u] \left(\frac{1}{r \{\cos \varphi\}^2} \frac{\partial \{\cos \varphi\}^2 [uv]}{\partial \varphi} + \frac{\partial [u\omega]}{\partial P} \right) dm}_c + \int f [u] [v] dm - \int [u] [F] dm \quad [12]$$

where r is the radius of the Earth, φ is the latitude, $[]$ indicates a zonal average, f is the Coriolis parameter, and dm is an increment of atmospheric mass. The subtropical jets have large contribution to the zonal component of KE: $[u]^2$ and the momentum flux $[uv]$ are modified by $\cos(\varphi)$ and $[u]$ factors that shift the larger values of the integrand (term c) to lower latitudes closer to the subtropical jet location.

The eddies need horizontal tilts to accomplish the observed momentum fluxes. Figure 10 illustrates the southwest to northeast tilts for poleward transport by Northern Hemisphere eddies.

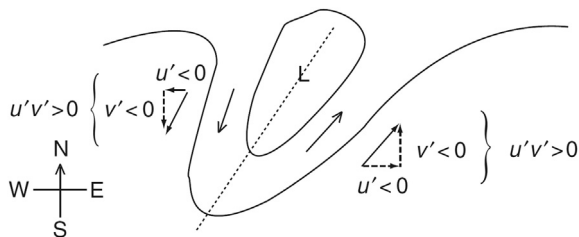


Figure 10 Schematic illustration of how a horizontal tilt of the trough axis (dotted line) leads to a net meridional transport of eddy zonal momentum. Primes denote winds with the zonal average removed. In this case the zonal average eddy momentum flux is northward. In contrast, a low that is symmetric about a north–south axis has $u'v'$ contributions on the east and west sides that cancel in the zonal mean.

Observed Energetics

Global Energy Balance

Ignoring seasonal heating and climatic change heating, there should be a balance between the solar energy absorbed by the Earth and that radiated away to space. The actual energy budget between the Earth and space depends on a variety of factors such as cloud cover, atmospheric composition, and surface properties. Estimates of energy fluxes for the Earth's surface and atmosphere on global and annual averages are presented in Figure 11.

Some limitations of this summary depiction are listed below:

1. The balance shown is global, so net radiation is zero. Net radiation (solar minus terrestrial) is positive from 38° N to 38° S and negative elsewhere.
2. Heat fluxes sustain the net radiation pattern; those motions are not included.
3. Vertical fluxes of heat and radiation are not shown, only the net transfer for the whole atmosphere.

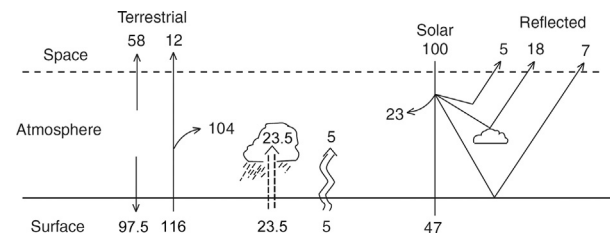


Figure 11 Global average energy balance expressed as percentages of the solar radiation striking the top of the atmosphere. Estimates of the solar constant vary, but the 100 units in the figure correspond to $\sim 341 \text{ W m}^{-2}$. Right side: solar radiation processes showing amounts reflected and absorbed. Middle: surface sensible heat flux (wavy arrow) and surface latent heat flux (dashed arrow). Left side: terrestrial radiation processes showing emission, transmission, and absorption. Data in the figure are based primarily on Trenberth, K., Fasullo, J., Kiehl, J., 2009. Earth's global energy budget. Bulletin of the American Meteorological Society 90: 311–323.

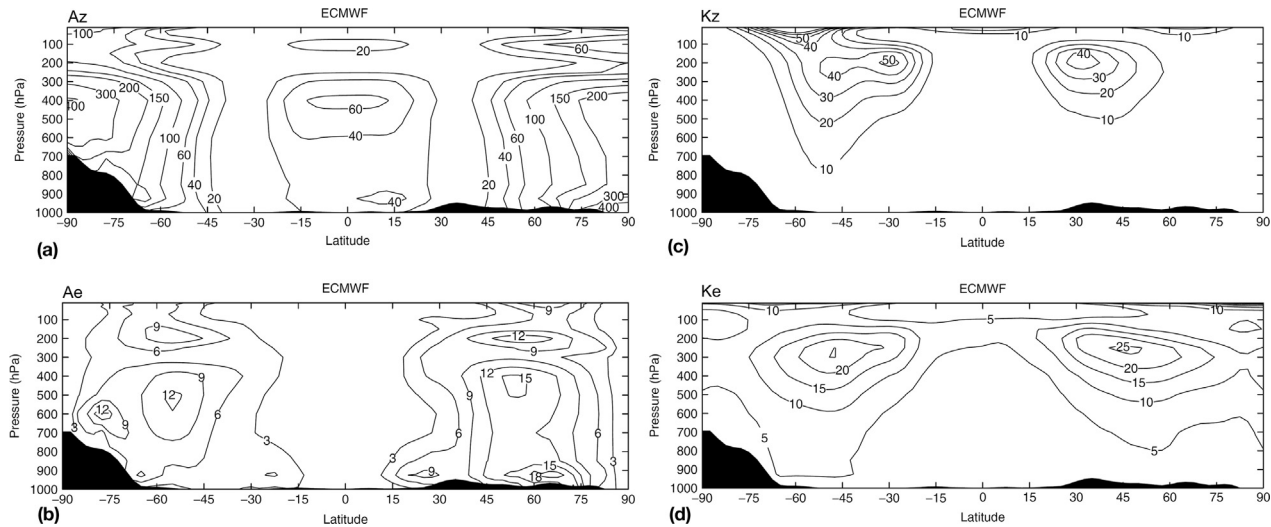


Figure 12 Zonal and annual average APE (a) of the zonal mean state, A_z , and (b) of the zonally varying state, A_e . Zonal and annual average KE (c) of the zonal mean flow, K_z , and (d) of the zonally varying flow, K_e . The units are $10^5 \text{ J m}^{-2} \text{ bar}^{-1}$. Reproduced from Marques, C., Rocha, A., Corte-Real, J., Castanheira, J., Ferreira, J., Melo-Gonçalves, P., 2009. Global atmospheric energetics from NCEP–Reanalysis 2 and ECMWF–ERA40 Reanalysis. *International Journal of Climatology*, 29: 159–174.

Figure 11 shows the following:

1. At the Earth's orbit, the longwave radiation from the Earth greatly exceeds the longwave radiation from the Sun. So, solar (shortwave) radiation can be treated separately from terrestrial (longwave) energy.
2. The (shortwave) albedo is greatly affected by clouds, which also strongly affect terrestrial emission.
3. More solar radiation is absorbed by the ground (47%) than by the air (23%).
4. The solar radiation reaching the ground evaporates water, is emitted as longwave radiation, or creates a sensible heat flux, in that order of (net) magnitude.
5. The net surface emission must balance the input (18.5 units) not lost by surface fluxes. However, the actual surface longwave emission (116 units) exceeds the shortwave input (47 units) because of downward radiation from the atmosphere, this means the surface temperatures are larger than expected from just the shortwave absorption, an increase known as the 'greenhouse' effect.
6. The average global annual energy absorbed is $\sim 235 \text{ W m}^{-2}$. Multiplied by the Earth's surface area, this is about 121 PW ($1.2 \times 10^{17} \text{ W}$).

The Energy Box Diagram

Since the tropical circulations are dominated by the zonal average Hadley circulation and the midlatitude weather is dominated by the zonally varying frontal cyclones, it is logical to partition the energy into zonal average and zonally varying (eddy) parts. The total APE can be partitioned into zonal average (A_z) and eddy (A_e) parts. Similarly, the total KE is partitioned into zonal average (K_z) and eddy (K_e) parts. These four categories of energy are shown in **Figure 12**. Zonal average of the APE in the zonal mean fields (**Figure 12(a)**) is large in the tropics and increases from a subtropical minimum to largest values at

the poles. The zonal average of APE from eddy structures is largest in the middle latitudes (**Figure 12(b)**). The zonal mean KE of the zonal mean flows (**Figure 12(c)**) has largest values in the middle latitudes where the major jet streams are found, including the dual jet in the Southern Hemisphere during local winter. The zonal mean KE from eddy motions (**Figure 12(d)**) is largest in the middle latitudes, with largest values in the upper troposphere. Compared with K_z the distribution of K_e is broader in the vertical and centered at higher latitudes. Comparison with **Figure 5** indicates that most of the tropopause level KE is in the zonal mean flow while in the middle and lower troposphere the KE is composed of approximately equal contributions from zonal mean and eddy flows.

The sources and sinks of energy discussed above can be summarized for the atmosphere using the 'box' diagram. Each box discussed here is a combination of zonal or eddy quantities that contribute to KE or APE. Other forms are possible, such as transient versus time mean or subdividing the eddies into different wave number groups. Arrows indicate input and output from each box as identified in the energy equations. Energy is converted back and forth between various forms, but only net changes are shown. The Hadley circulation is contained in the zonal mean quantities at the top row of the box diagram. Midlatitude frontal cyclones are included in the bottom row. The box diagram has some limitations:

1. The diagram only refers to global mean properties. For example, A_z to A_e is largest mainly in middle latitudes.
2. Only net changes are shown, whereas large regional variations occur. A_z to $K_z > 0$ for the Hadley cells but < 0 for Ferrel cells. Some studies show the global value of this conversion as negative.
3. Some conversions are simultaneous, as mentioned above, especially the A_z to A_e to K_e route by which frontal cyclones intensify. The small size of the A_z to K_z conversion hides a redundant geostrophic and hypsometric link between A_z and K_z .

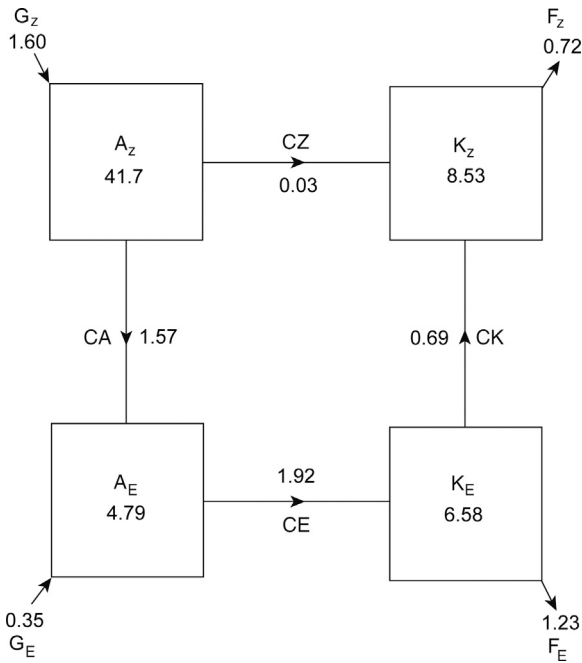


Figure 13 Energy ‘box’ diagram showing reservoirs of zonal mean APE (A_z) and KE (K_z); eddy APE (A_E) and KE (K_E) in the same orientation as Figure 12. Also shown are net energy conversions (CA, CE, CK, CZ); and net diabatic generation or destruction. Global and annual average values indicated. The reservoirs are in units of 10^5 J m^{-2} and the conversions and diabatic processes have units of watts per square meter. The conversions are given letter labels for future reference. The numbers for A_z and A_E are somewhat arbitrary, but consistent with each other. The values are redrawn from Marques et al. (2009) and based on ERA-40 data from 1979 to 2001. Marques, C., Rocha, A., Corte-Real, J., Castanheira, J., Ferreira, J., Melo-Gonçalves, P., 2009. Global atmospheric energetics from NCEP–Reanalysis 2 and ECMWF–ERA40 Reanalysis. International Journal of Climatology 29: 159–174.

4. Some conversions are hard to measure directly and are sometimes approximated (e.g., A_z to K_z) or deduced as a residual (e.g., G_E and A_E to K_E).
5. The box diagram gives arbitrary if not misleading results for certain situations of wave–mean flow interaction.

Observed reservoirs, conversions, sources, and sinks of energy are depicted in Figure 13. Diabatic processes create much A_z which in turn drives K_z of zonal mean circulations such as the Hadley cells and the zonal mean midlatitude westerlies. Some A_z is converted into A_E which becomes K_E especially in midlatitude frontal cyclones. Convergence of eddy momentum is a net conversion of K_E to K_z . Since friction removes K_E there must be net A_E to K_E conversion. Depending on the estimated strength of eddy frictional loss: F_E , eddy APE generation: G_E may be negative.

The box diagram for global energy shows the following:

1. While the total value of the APE is somewhat arbitrary, the relative sizes of similar energy ‘reservoirs’ are worth noting. For example, K_E is almost half of the total KE. A_E is about a tenth of the total APE.

2. The flow of energy consists primarily of G_z to A_z to A_E to K_E to F_E . However, the small conversion CZ can be misleading since there is some arbitrariness in how the conversions are defined as will be discussed below.
3. Different phenomena follow different paths. The A_z to K_z relates to the Hadley cell in terms of Figure 3. Baroclinic instability is A_z to A_E to K_E and obviously a primary track in the diagram. Barotropic instability is K_z to K_E and it is clearly negative (eddies feed KE into the zonal mean flow).

Transformed Eulerian Mean (TEM) and Stratospheric Energy Box Diagram

An alternative energy analysis can be constructed in a TEM framework based on an ‘eddy-induced circulation’ that results (in large part) from eddy heat fluxes. The purpose of the residual circulation is to simplify the net effect of the eddies on the mean flow in part by including their contribution to a zonal mean meridional circulation. The residual circulation (*subscripts) might be defined as

$$[v_*] = [v] - \frac{1}{p} \frac{\partial}{\partial z} \left(p \frac{[v' \theta']}{\partial [\theta]} \right) \quad [w_*] = [w] + \frac{\partial}{\partial y} \left(p \frac{[v' \theta']}{\partial [\theta]} \right) \quad [13]$$

The TEM formalism is applied more commonly to understand the stratospheric general circulation than the tropospheric. One reason is that the divergence of Eliassen-Palm flux term in the zonal momentum equation has a lot of cancelation with the flux of planetary angular momentum by the TEM residual circulation. For stratospheric planetary waves, the residual circulation induced by eddy heat flux convergence exceeds that from the diabatic heating, but that does not hold for the troposphere, in part due to the lower boundary.

If there is nonacceleration, then there is no net gain of energy in the different ‘energy boxes.’ But in some non-acceleration situations the ‘conventional’ formulation of the previous section has transfers of energy, though they are such that energy input to a ‘reservoir’ equals energy output. The transfers of energy could be viewed as misleading, since there is no net generation or destruction despite the large conversions with adjacent reservoirs. Under the same nonacceleration assumption, the energy conversions are all zero in the TEM formulation. While that might seem superior, problems arise when the nonacceleration condition is not met such as for growing baroclinic waves.

The definitions of the energy conversions differ between the TEM and conventional formulations. The TEM formulation does not allow the CA conversion, instead, energy is exchanged between waves and zonal mean through a CK conversion. However, in the TEM formulation the conversion between zonal and eddy KE is related to the Eliassen–Palm flux, which in turn is a vector that depends on eddy momentum and eddy heat fluxes.

When considering the stratosphere alone, a new source or sink of KE arises from the work done by deformation of the tropopause. These boundary fluxes are substantial and a major driver for planetary-scale stratospheric circulations. In a conventional energy cycle depiction (like Figure 13) the energy conversions would appear large, but largely go in a loop: K_z to A_z

to A_E to K_E and back to K_z in the stratosphere during winter. So, much of the large conventional energy conversions do not result in corresponding large net gain or loss of energy in the individual components. The same situation in the TEM framework shows mechanical forcing of K_z , most of which is transferred to K_E and then to A_E , where it is lost by diabatic cooling. The TEM framework is more clear than the conventional view, though it might be more physically reasonable to have a direct forcing of the stratospheric K_E by the tropospheric longest waves instead of going through K_z first. During summer, in the stratosphere the eddies transport heat poleward making the polar region warmer than it would be from local radiative balance (geometry makes the incident solar radiation larger at the pole than at the adjacent middle latitudes), so the presence of the eddies results in polar radiative net cooling instead of net warming and the energy flow is from eddies to zonal mean.

Column Average Energetics

Vertically integrating the combination of the temperature conservation and KE equations yields

$$\begin{aligned} \frac{1}{g} \frac{\partial}{\partial t} \int_0^{P_s} (C_p T + \Phi_S + KE) dP \\ = -\frac{1}{g} \nabla_H \cdot \int_0^{P_s} (C_p T + \Phi + KE) V_H dP + Q_h + Q_f \end{aligned} \quad [14]$$

Subscript H indicates the horizontal components, KE is defined in eqn [1], and Φ_S is the surface geopotential. Q_h contains the net diabatic heating terms from the temperature conservation equation: net downward radiation at the top of the atmosphere, surface heat flux, and precipitation rate, all expressed as a heating rate. Q_f is heating due to friction (which is very small, $\sim 2 \text{ W m}^{-2}$). Vertically integrating the moisture conservation equation yields

$$\frac{L}{g} \frac{\partial}{\partial t} \int_0^{P_s} q dP = -\frac{L}{g} \nabla_H \cdot \int_0^{P_s} q V_H dP - Q_w \quad [15]$$

where Q_w is the difference in precipitation minus surface evaporation rates in the atmosphere, expressed as a heating rate. Combining the two previous equations gives an equation for a type of TE that includes internal, potential, kinetic, and latent energy:

$$\begin{aligned} \frac{1}{g} \frac{\partial}{\partial t} \int_0^{P_s} (C_p T + \Phi_S + KE + Lq) dP \\ = -\frac{1}{g} \nabla_H \cdot \int_0^{P_s} (C_p T + \Phi + KE + Lq) V_H dP + Q_h + Q_f - Q_w \end{aligned} \quad [16]$$

Hence, vertical and horizontal advectons of MSE + KE are balancing the diabatic processes. A similar balance, between radiative cooling and adiabatic warming of sinking air, was exploited for the Carnot cycle model of the Hadley cell discussed above. Ignoring the tiny Q_f , eqn [14] shows that Q_h is proportional to a divergence of the flux of the combination DSE + KE. Similarly, from eqn [16] $Q_h - Q_w$ is proportional to the divergence of the TE. Hence, those fluxes can be deduced from the Q_h and $Q_h - Q_w$ fields and reveal large-scale flows of energy within the atmosphere.

Figure 14 shows the distribution of Q_h and Q_w for the extreme seasons; the total diabatic energy sources and sinks ($Q_h - Q_w$) are subdivided into quasistationary and transient contributions along with the corresponding energy fluxes. Figure 14 shows the following:

1. Q_h has strong sources in regions with heavier precipitation such as the ICZ, south Pacific convergence zone (SPCZ), and winter midlatitude frontal cyclone storm tracks. Strong surface sensible heat flux over WBCs also amplifies the Q_h .
2. Q_h is a strong sink: over winter continents due to intense radiative cooling and the eastern subtropical oceans due to negative net radiation.
3. Q_w has maxima where there is net precipitation (ICZ, SPCZ, and midlatitude winter storm tracks) and minima where there is greater net evaporation (subtropical oceans). Evaporation exceeds precipitation more strongly during winter in the subtropics. The moisture fluxes are out of the subtropics toward the ICZ, SPCZ, and midlatitude storm tracks.
4. The slowly varying diabatic sources of TE, $Q_h - Q_w$ are shown in Figure 14(c) and 14(g). The sources of TE are areas of strong evaporation over the subtropical and tropical oceans. Precipitation does not enter into eqn [16] because the flux (and hence conservation) of MSE means that latent heating is compensated by adiabatic cooling of the rising air, such as in the ICZ. Strong surface heat fluxes (and some evaporation) occur over the WBCs during winter. (During summer there is a sink over the WBCs.) During winter there is a sink of TE at higher latitudes due to the strong negative net radiation, with some enhancement of the sink over the continents.
5. The flow of TE for monthly mean and longer features is from the tropics, subtropics, and WBCs toward the higher latitudes in the vertical mean. However, for the Hadley cell, it has to be transported first equatorward, then upward, and then poleward, including phase changes of the water.
6. The faster varying diabatic sources of TE: $Q'_h - Q'_w$ (Figure 14(d) and 14(h)) are generally along the equatorial side of the midlatitude storm tracks with greater intensity during winter months. The sink tends to be immediately poleward of the storm tracks, a pattern reinforced by the TE flux.
7. The flux of TE is greatest where the $Q_h - Q_w$ gradient is greatest. The peak is in the middle latitudes ($\sim 40^\circ$ latitude) with peak value of $\sim 5 \text{ PW}$. The ocean transports heat as well, though peak values amount to $\sim 1/4$ (Northern Hemisphere) to $\sim 1/10$ (Southern Hemisphere) of the transport by the atmosphere.

Summarizing the Energy Cycle

Energy in the general circulation follows paths from sources to sinks. Energy is mathematically cast in several useful forms and it is linked to several global constraints. To provide an overview of these diverse properties, Table 1 and Figure 15 summarize how energy in kinetic and potential forms flows in the general circulation. Heat and APE are similar concepts and are compared in the table and figure. Similarly, momentum and KE may be considered together. The table and figure make clear that heat and momentum have similar circuits.

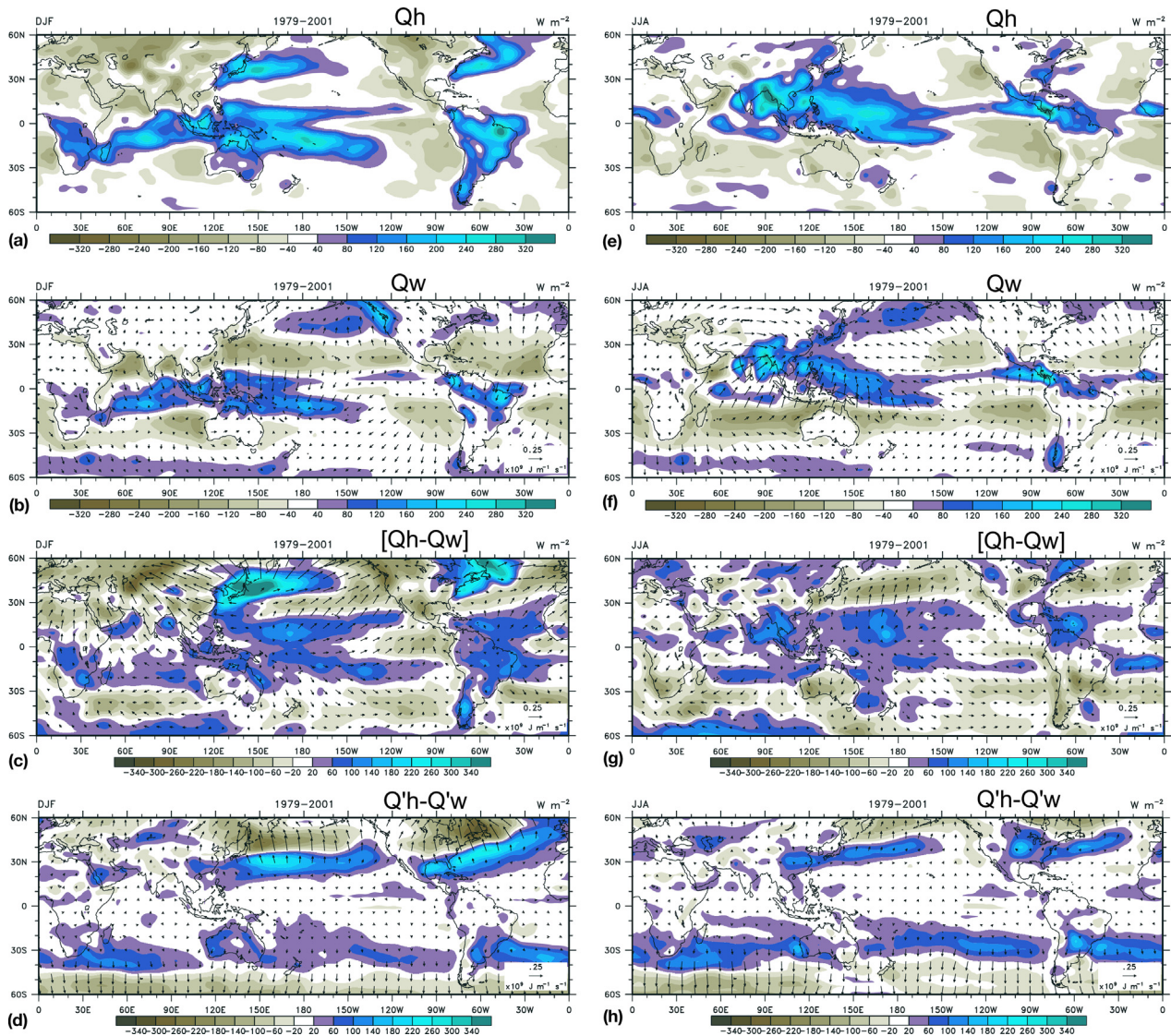


Figure 14 Vertically integrated components of the energy flow during December–February (left column) and June–August (right column) using data from 1979–2001. (a) and (e) are net diabatic heating. (b) and (f) are moisture sources and sinks (contoured) and the implied net transport (vectors). (c) and (g) are TE change (contours) and net energy fluxes (vectors) due to ‘quasistationary’ processes varying on monthly mean or longer timescales. (d) and (h) are similar to (c) and (g) but for ‘transient’ processes varying faster than monthly mean timescales. The sources and sinks are all expressed as energy fluxes with units of watts per square meter. The vector scales and units are indicated with a reference vector in the lower right corner of individual panels. Reproduced from Trenberth, K., Stepaniak, D., 2004. The flow of energy through the earth’s climate system. *Quarterly Journal of the Royal Meteorological Society*, 130: 2677–2701.

Table 1 Stages in the APE (heat) and KE (momentum) energy cycle

APE or heat flow	KE or momentum flow
1. Solar and terrestrial radiation create excess heating in the tropics and a deficit poleward of 38°	1. Westerly momentum is introduced in the tropics and is removed by friction in midlatitudes.
2. Result of item (1) is a poleward heat flux.	2. Result of item (1) is a poleward westerly momentum flux.
3. In midlatitudes eddies are the main mechanism for heat transport.	3. In midlatitudes eddies are the main mechanism for momentum transport.
4. The CA and CE conversions (see Figure 13) show that horizontal and vertical heat fluxes create eddy energy (baroclinic process). Latent heat release may also contribute.	4. Eddy momentum fluxes also provide sources and sinks of eddy KE from the CK conversion (see Figure 13). Since global average CK is positive, eddies must lose KE to the mean flow in the net (barotropic process).
5. Net radiation being positive causes the heat flux to increase with latitude in the subtropics. (More and more heat must be transported poleward to maintain quasisteady PE.)	5. The flux of zonal mean KE keeps increasing with latitude in the subtropics where CK is positive. (More and more momentum must be transported poleward to maintain quasisteady KE.)
6. The eddy heat flux is down the T gradient.	6. Eddy momentum flux is up the gradient of $[u]\cos^{-1}\phi$ at many latitudes.
7. The heat flux is maximum where net radiation is zero.	7. The flux of (KE) reaches a maximum where CK equals zero.
8. Poleward of the heat flux maximum there is cooling by net radiation.	8. Poleward of the angular velocity, $[u]\cos^{-1}\phi$, maximum, eddies remove energy from (KE) in the net.

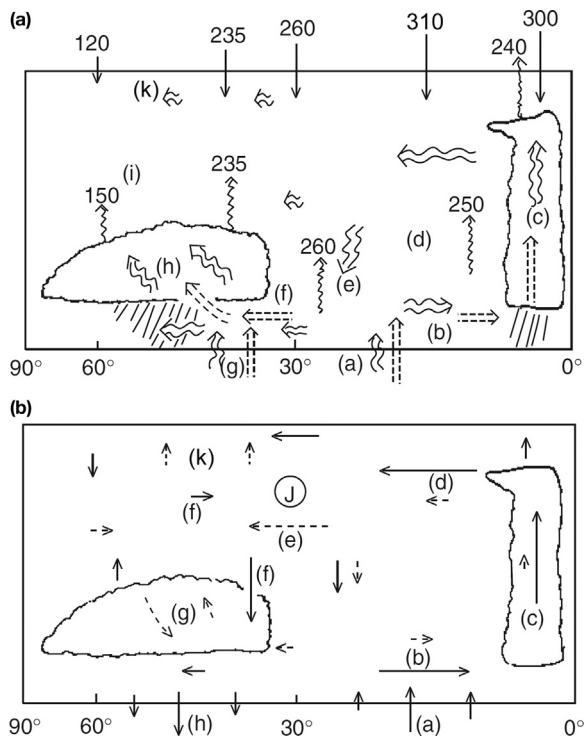


Figure 15 (a) Schematic meridional cross sections of the atmospheric cycles of (a) APE and heat and (b) KE and momentum. Arrow lengths are intended to suggest relative magnitudes. In panel (a) single-shafted arrows depict radiation (straight for absorbed solar; wavy for terrestrial emitted to space) with representative numerical values given in watts per square meter. Double-shafted arrows depict heat fluxes (dashed for latent; wavy for sensible heat). Letters correspond to distinct parts of the cycle. Solar radiation (a) is absorbed in the tropics and subtropics, then that heat energy is transported (b) equatorward. Latent heat (c) is converted into sensible heat in the ICZ then transported poleward (d) in the upper troposphere. Sinking in the Hadley cell (e) brings heat downward. Eddy fluxes (f) extract heat from the subtropics and are augmented by surface fluxes (g) at WBCs. Heat is mixed upward vertically (h) in frontal cyclones, whereupon a net loss occurs to space (i). A weak poleward flux (k) results from the eddy-induced stratospheric circulation. In panel (b), momentum transport in the troposphere is separated into mean meridional cells (solid arrows) and eddies (dashed arrows). Letters correspond to these parts of the cycle: Slowing down surface easterlies imparts westerly momentum (a) into the tropical boundary layer. That momentum is transported equatorward (b) then upward (c) in the ICZ convection. The upper Hadley cell transports the momentum (d) poleward. Eddies further transport the momentum (e) poleward, out of the subtropics, while the Ferrel cell (f) both opposes the eddy flux and mixes some momentum downward. Frontal cyclones also have a net downward mixing (g) of westerly momentum (e.g., behind cold fronts) that is lost by friction at the surface (h). The transport creates westerly momentum convergence in the subtropics and midlatitudes forming a subtropical jet (J) and a KE maximum there, (k) and other arrows in the stratosphere are meant to indicate mechanical forcing by the midlatitude ultralong waves and by deep tropical convection.

Westerly momentum is defined positive, so frictional slowing of easterlies in the tropical boundary layer is a *source* of westerly momentum but a *sink* of KE. The low-level flow in the Hadley cells gains westerly momentum and transports it equatorward. Surface fluxes of heat and water provide a diabatic source of warmth and moisture to air parcels as they approach the ICZ.

In the ICZ, westerly momentum is transported to the upper troposphere. Latent heat is released where the efficiency factor is large and positive, leading to strong diabatic generation of APE. While the precipitation does not contribute directly to the TE generation, it does reinforce the equatorward pressure gradient that drives the upper level Hadley cell motion, establishes the westerlies, and creates other indirect impacts.

The upper branch of each Hadley cell transports westerly momentum poleward. Conservation of angular momentum builds the velocity relative to the Earth's surface, i.e., creating KE and providing one mechanism to create the subtropical jets. The poleward extent of the motion arises from interaction between the (poleward) pressure gradient force and the Coriolis force (at a right angle to the motion); these two forces would accelerate parcels along a trochoidal path. Because the MSE of the poleward moving air is much greater than the MSE of the equatorward moving air below, the Hadley cell has a net poleward transport of heat.

The subtropical oceans are where much energy is input into the atmosphere through evaporation. The subtropics are also a transition between the convection-dominated tropical circulations and the frontal cyclone-dominated midlatitude circulations. Negative net radiation encourages parcels in the Hadley cell to sink, bringing down some westerly momentum as well as high potential temperatures. The frontal cyclones mix momentum and heat vertically. The vertical fluxes of heat by each cyclone and the vertical shear of the jet streams both are fundamental parts of the baroclinic instability mechanism.

In middle latitudes, air in the cyclones' warm sector has a poleward component of motion, while air in the cold sector moves equatorward: in both sectors *eddy* heat transport is poleward. Much precipitation accompanies the frontal cyclones with the bulk of it occurring in the warm sector, so there may be diabatic generation of eddy APE but loss of zonal APE. Further poleward, radiative cooling, especially from cloud tops, generates APE. Mature frontal cyclones develop momentum fluxes that converge upper level westerly momentum, while their heat fluxes reduce the meridional temperature gradient on a zonal average. To maintain thermal wind balance a secondary circulation forms which also transports momentum (equatorward at upper levels). The westerly momentum mixed to the surface (for example, in subsiding air of cold sectors) is removed by friction in the boundary layer, becoming a sink of westerly momentum and of KE.

In the stratosphere, there is input of mechanical (kinetic) energy by tropical convection and by midlatitude long waves as well as heating as ozone absorbs radiation. The eddy-induced circulation transports some heat poleward though angular momentum is mixed vertically and horizontally.

See also: Climate and Climate Change: Energy Balance Climate Models. **Dynamical Meteorology:** Balanced Flow; Baroclinic Instability; Overview; Quasigeostrophic Theory. **General Circulation of the Atmosphere:** Mean Characteristics. **Land-Atmosphere Interactions:** Overview. **Middle Atmosphere:** Transport Circulation. **Numerical Models:** General Circulation Models. **Stratosphere/Troposphere Exchange**

and Structure: Global Aspects. **Thermodynamics:** Moist (Unsaturated) Air. **Tropical Meteorology and Climate:** Hadley Circulation.

Further Reading

- Dutton, J., Johnson, D.R., 1967. The theory of available potential energy and a variational approach to atmospheric energetics. In: *Advances in Geophysics*, Vol. 12. Academic Press, New York, NY. 333–436.
- Grotjahn, R., 1993. *Global Atmospheric Circulations: Observations and Theories*. Oxford University Press, New York, NY.

- James, I., 1994. *Introduction to Circulating Atmospheres*. Cambridge University Press, Cambridge, UK.
- Karoly, D.J., Vincent, D.G., 1998. *Meteorology of the Southern Hemisphere*. American Meteorological Society, Boston, MA.
- Peixoto, J.P., Oort, A.H., 1992. *Physics of Climate*. American Institute of Physics, New York, NY.
- Trenberth, K.E., Stepaniak, D.P., 2004. The flow of energy through the Earth's climate system. *Quarterly Journal of the Royal Meteorological Society* 130, 2677–2701.